Development 127, 1691-1702 (2000)
Printed in Great Britain © The Company of Biologists Limited 2000
DEV1501

Zebrafish *Mesp* family genes, *mesp-a* and *mesp-b* are segmentally expressed in the presomitic mesoderm, and Mesp-b confers the anterior identity to the developing somites

Atsushi Sawada[1], Andreas Fritz[2], Yun-Jin Jiang[3], Akihito Yamamoto[4,‡], Kyo Yamasu[5], Atsushi Kuroiwa[1], Yumiko Saga[6] and Hiroyuki Takeda[1,*]

[1]Division of Biological Science, Graduate School of Science, Nagoya University, Chikusa-ku, Nagoya 464-8602, Japan
[2]Department of Biology, Emory University, 1510 Clifton Road, Atlanta, GA 30322, USA
[3]Vertebrate Development Laboratory, Imperial Cancer Research Fund, 44 Lincoln's Inn Fields, London WC2A 3PX, UK
[4]Howard Hughes Medical Institute, Department of Biological Chemistry, University of California, Los Angeles, CA 90095-1662, USA
[5]Department of Regulation Biology, Faculty of Science, Saitama University, Urawa, Shimo-Okubo, Saitama 338-8570 Japan
[6]Cellular and Molecular Toxicology, National Institute of Health Sciences, Kamiyohga, Setagaya-ku, Tokyo 158-8501 Japan
‡Present address: Institute of Molecular Embryology and Genetics, Kumamoto University School of Medicine, Kumamoto 860, Japan
*Author for correspondence at present address: Division of Early embryogenesis, National Institute of Genetics, Mishima, Shizuoka 411-8540, Japan
e-mail: htakeda@lab.nig.ac.jp

Accepted 1 February; published on WWW 21 March 2000

SUMMARY

Segmentation of a vertebrate embryo begins with the subdivision of the paraxial mesoderm into somites through a not-well-understood process. Recent studies provided evidence that the Notch-Delta and the FGFR (fibroblast growth factor receptor) signalling pathways are required for segmentation. In addition, the Mesp family of bHLH transcription factors have been implicated in establishing a segmental prepattern in the presomitic mesoderm. In this study, we have characterized zebrafish *mesp-a* and *mesp-b* genes that are closely related to *Mesp* family genes in other vertebrates. During gastrulation, only *mesp-a* is expressed in the paraxial mesoderm at the blastoderm margin. During the segmentation period, both genes are segmentally expressed in one to three stripes in the anterior parts of somite primordia. In *fused somites* (*fss*) embryos, in which all early somite boundary formation is blocked, initial *mesp-a* expression at the gastrula stage remains intact, but the expression of *mesp-a* and *mesp-b* is not detected during the segmentation period. This suggests that these genes are downstream targets of *fss* at the segmentation stage. Comparison with *her1* expression (Müller, M., von Weizsäcker, E. and Campos-Ortega, J. A. (1996) *Development* 122, 2071-2078) suggests that, like *her1*, *mesp* genes are not expressed in primordia of the first several somites. Furthermore, we found that zebrafish *her1* expression oscillates in the presomitic mesoderm. The *her1* stripe, which first appears in the tailbud region, moves in a caudal to rostral direction, and it finally overlaps the most rostral *mesp* stripe. Thus, in the trunk region, both *her1* and *mesp* transcripts are detected in every somite primordium posterior to the forming somites.

Ectopic expression of Mesp-b in embryos causes a loss of the posterior identity within the somite primordium, leading to a segmentation defect. These embryos show a reduction in expression of the posterior genes, *myoD* and *notch5*, with uniform expression of the anterior genes, *FGFR1*, *papc* and *notch6*. These observations suggest that zebrafish *mesp* genes are involved in anteroposterior specification within the presumptive somites, by regulating the essential signalling pathways mediated by Notch-Delta and FGFR.

Key words: Segmentation, Somitogenesis, Notch signalling, *fused somites*, *Mesp2*, Zebrafish

INTRODUCTION

During vertebrate embryonic development, the paraxial mesoderm is subdivided into metameric subunits called somites. The somites are the first segmented structures to form during embryogenesis and they govern the metamerism of all somite-derived tissues; axial skeleton, the dermis of the back, and all striated muscle of the adult body (Christ and Ordahl, 1995) and spinal ganglia (Keynes and Stern, 1984). Individual pairs of somites, located symmetrically on either side of the neural tube, are formed in a rostrocaudal progression within the presomitic mesoderm (PSM). It is believed that the process of somitogenesis can be divided into three distinct stages, which may be regulated by different genetic mechanisms (Tam and Trainor, 1994). (1) Specification as paraxial mesoderm: the mesoderm derived from the primitive streak in mice and chick, the marginal zone in amphibians, and germ ring in fish or the tailbud, is arranged on both sides of the neural tube as

the paraxial mesoderm; (2) segmentation: the paraxial (somitic) mesoderm generates each segmental border and is divided into the so-called epithelial somites; (3) differentiation: the somites differentiate into the sclerotome and dermomyotome which subsequently segregates into the dermatome and myotome.

Recently, signalling molecules such as Shh, BMP and Noggin have been identified and implicated in patterning and differentiation within the somites (for review see Currie et al., 1998). Molecular and genetic analyses of zebrafish *no tail* (*ntl*), *floating head* (*flh*) and *spadetail* (*spt*) mutants have shed light on the mechanism underlying a cell fate decision between axial and paraxial mesoderm (Halpern et al., 1997; Talbot et al., 1995; Amacher et al., 1998).

The mechanisms of segmentation have been studied most extensively in chick embryos. Transplantation experiments in chick have shown that the anteroposterior subdivision within the somite, which has already been established during segmentation period (Stern and Keynes, 1987; Aoyama and Asamoto, 1988), serves to maintain the segmental arrangement of the somite. The understanding of the mechanisms that establish a segmental prepattern in the PSM has been greatly advanced in the last few years. The remarkably cyclic expression pattern of *c-hairy1*, a chick bHLH transcription factor, related to the *Drosophila* pair-rule gene *hairy*, in the PSM suggests the presence of an intrinsic molecular clock before the appearance of the somite (Palmeirim et al., 1997). Furthermore, the unique expression pattern of zebrafish *her1*, more distantly related to *hairy*, suggested a pair-rule prepattern in zebrafish PSM: it is expressed in two or three stripes demarcating the primordia of the odd numbered somites beginning with the 5th somite (Müller et al., 1996). Recent genetic analyses further indicate that segmentation of the PSM involves a cell-cell interaction mediated by the Notch receptors and their ligands. For example, segmental defects are seen in mouse embryos with a targeted inactivation of the genes encoding Dll1 (Hrabe de Angelis et al., 1997), Notch1 (Conlon et al., 1995), lunatic fringe (Zhang and Gridley, 1998; Evrad et al., 1998), and a component of the Notch-Delta signalling pathway called RBP-Jk or Su (H) (Oka et al., 1995). Recently, a dynamic expression pattern has been demonstrated for *lunatic fringe* in chick and mouse PSM, which resembles *c-hairy1* expression, suggesting a link between the segmentation clock and the Notch signalling pathway (McGrew et al., 1998; Forsberg et al., 1998; Aulehla and Johnson, 1999; del Barco Barrantes et al., 1999). Segmental defects are also detected in mice deficient in *fibroblast growth factor receptor1 (FGFR1*; Deng et al., 1994; Yamaguchi et al., 1994). Furthermore, recent experiments with zebrafish suggest a role of Eph signalling in segmentation (Durbin et al., 1998). All these genes are expressed in the PSM and implicated in early steps of somitogenesis.

Murine MesP1 and MesP2 are bHLH transcription factors (Saga et al., 1996, 1997) and they show a segmental expression pattern in the PSM. *Mesp2*-deficient mice showed two major defects during somitogenesis: a failure of the initiation of segmentation, and a disturbance of the somitic anteroposterior polarity. Recently, *Mesp*-related genes were cloned in chick (*cMeso-1*; Buchberger et al., 1998) and *Xenopus* (*Thylacine*; Sparrow et al., 1998; *Mespo*; Joseph and Cassetta, 1999). Like murine *Mesp* genes, they are predominantly expressed in the PSM, and both antisense and overexpression experiments suggest they have roles in segmentation. The exact nature of their role, and how their expression is regulated are important issues for understanding how paraxial mesoderm is segmented in different vertebrate species.

In this paper, we describe two zebrafish *Mesp*-related genes, *mesp-a* and *mesp-b*. Their expression in the PSM is confined to the anterior halves of presumptive and/or forming somites and is regulated by *fss* (van Eeden et al., 1996). Two-colour in situ hybridization with *mesp* and *her1* probes suggests that, like *her1*, *mesp-a* is not expressed in the cells that will contribute to the first several somites, supporting an idea of a difference between rostral and caudal somite formation (reviewed in Jiang et al., 1998). Furthermore, we found that the newly established expression domain of *her1*, near the tailbud, travels (or moves) anteriorly and finally overlaps the *mesp* expression domain. Thus, like *mesp*, *her1* transcripts are detected in every somite primordium (except for the first several ones) preceding boundary formation. Finally, ectopic expression experiments suggest that Mesp-b is involved in establishing the anterior fate within the presumptive somites.

MATERIALS AND METHODS

Fish embryos

All studies on wild-type zebrafish (*Danio rerio*) were carried out in the Oregon AB background. The mutant alleles used in this paper are *fused somites* (*fss^{ti1}*), *beamter* (*bea^{tw212b}*), *deadly seven* (*des^{th35b}*), *after eight* (*aei^{tr233}*) and *mindbomb* (*mib^{ta52b}*). Embryos obtained from natural crosses were maintained in 1/3 Ringer's solution (39 mM NaCl, 0.97 mM KCl, 1.8 mM $CaCl_2$, 1.7 mM Hepes at pH 7.2) at 28.5°C and staged according to age (hours postfertilization at 28.5°C) and morphological criteria (Kimmel et al., 1995).

Isolation of zebrafish *mesp-a* and *mesp-b* genes

Degenerate oligonucleotide primers were designed for the amino acid sequences conserved between MesP1 and MesP2 proteins. A sense primer (5′ GA(AG)(AC)G(AGCT)GA(AG)AA(AG)(CT)T(AGCT)-(AC)G 3′) encoding the amino acid sequence EREKLR and an antisense primer (5′ (GC)(AT)(AGCT)A(AG)(AG)TG(AGCT)CC-(AGT)AT(AG)TA 3′) encoding the amino acid sequence YIGHLS were used for amplification.

Total RNA from the shield-stage embryos was prepared by the acid guanidium thiocyanate/phenol/chloroform extraction method (Chomczynski and Sacchi, 1987). First-strand cDNA was synthesized by using 10μg of total RNA and oligo-dT primer (RTG cDNA synthesis kit, Pharmacia). For PCR, 1/10 volume of the first-strand cDNA was used for PCR amplification. One fragment gave an unexpected large product which hybridized with the murine *Mesp1* probe. The fragment was then cloned into pBluescript II SK+ (Stratagene) and sequenced. The fragment was found to contain the bHLH region similar to that of murine MesP1 as well as the 3′ entire UTR of the gene. This cDNA was designated as zebrafish *mesp-a*. The 5′ fragment was obtained using a CapFinder^{TM} PCR cDNA Library Construction Kit (CLONETECH Laboratories, Inc. Palo Alto, CA). During the course of the study, we screened a PAC genomic library and we found a PAC clone that contained both *mesp-a* and a second *Mesp*-related gene. From the partial sequence of this clone, we isolated a complete cDNA clone of the second gene by PCR. The second *Mesp*-related gene was designated as *mesp-b*. Sequences of the two *Mesp*-related cDNAs were determined by comparing sequence data from two independently amplified clones to exclude PCR errors.

RNA injection

All capped sense RNAs were synthesized and purified as previously described (Makita et al., 1998; Koshida et al., 1998). The synthesized mRNAs were diluted to the appropriate concentration with distilled water and injected into 1-cell stage embryos. The concentration used for each RNA was as follows: 0.1 μg/μl for *mesp* genes, 0.1 mg/ml for *green fluorescent protein* (*GFP*); 0.1 μg/μl for *lacZ* (except for the samples shown in Fig. 5E-H in which 0.02 μg/μl of *lacZ* RNA were coinjected). Approximately 400-500 pl of diluted RNA was injected into each embryo.

β-galactosidase staining in *lacZ*-injected embryos

The embryos injected with *lacZ* RNA were fixed with 4% paraformaldehyde in PBS for 30 minutes at room temperature. They were washed 4 times with PBST for 10 minutes each time and washed once with buffer A (17.5 mM $K_3[Fe(CN)_6]$, 17.5 mM $K_4[Fe(CN)_6]$, 1 mM $MgCl_2$ in PBS) for 10 minutes. Colour staining was performed using 0.4 mg/ml dilution of X-gal in buffer A for 2 hours at 37°C. They were washed three times with PBST for 5 minutes each time and refixed with 4% paraformaldehyde in PBS at 4ºC overnight. The embryos were then processed for in situ hybridization.

In situ hybridization

Single colour in situ hybridization was carried out as described by Koshida et al. (1998). Two-colour in situ hybridization was performed essentially as described by Jowett and Yan (1996). Briefly, one antisense RNA probe was labeled with digoxigenin-UTP (Roche) and the other was labeled with fluorescein-UTP (Roche). Hybridization was performed with both probes to the embryos simultaneously. After reaction with anti-fluorescein alkaline phosphatase Fab fragments at 4ºC overnight, colour staining was performed with Fast Red (Roche). Then, alkaline phosphatase was inactivated by incubation with 0.1 M glycine-HCl (pH 2.2), 0.1% Tween 20 twice for 15 minutes each time at room temperature. After washing with MABT (100 mM maleic acid, 150 mM NaCl, 0.1% Tween 20) 4 times for 5 minutes each time, the embryos were fixed with 4% paraformaldehyde in PBS for 20 minutes at room temperature. The samples were washed 5 times with MABT for 5 minutes each time, and reacted with anti-digoxigenin alkaline phosphatase Fab fragments at 4C overnight. Second colour staining was performed with BM purple (Roche) or ELF^{TM}-97 mRNA In Situ Hybridization Kit (Molecular Probes).

RESULTS

Isolation of two zebrafish *Mesp*-related genes

A partial cDNA fragment of a zebrafish *Mesp*-related gene was obtained from shield stage cDNAs by PCR with degenerate primers corresponding to the bHLH region of murine *Mesp1*. The cDNA fragment contained the *Mesp*-related bHLH region and was designated as *mesp-a*. The second related gene, *mesp-b*, was obtained from somite-stage cDNA by PCR. The primers used were designed based on a partial sequence of a DNA fragment derived from a PAC clone containing *mesp-a*. The *mesp-a* cDNA, which consists of 887 base pairs (bp), encodes a protein of 223 amino acids from the first possible initiation site at the 24th nucleotide (nt) (Fig. 1A). Similarly, translation from the ATG at the 13th nt in the 930 bp *mesp-b* cDNA will yield a protein of 236 amino acids (Fig. 1A). The sequences surrounding the first in-frame methionine have a good match to the Kozak consensus (Kozak, 1987) and hence this is most likely to be the translation initiation site. The bHLH domains of these two proteins share more than 90% amino acid identity

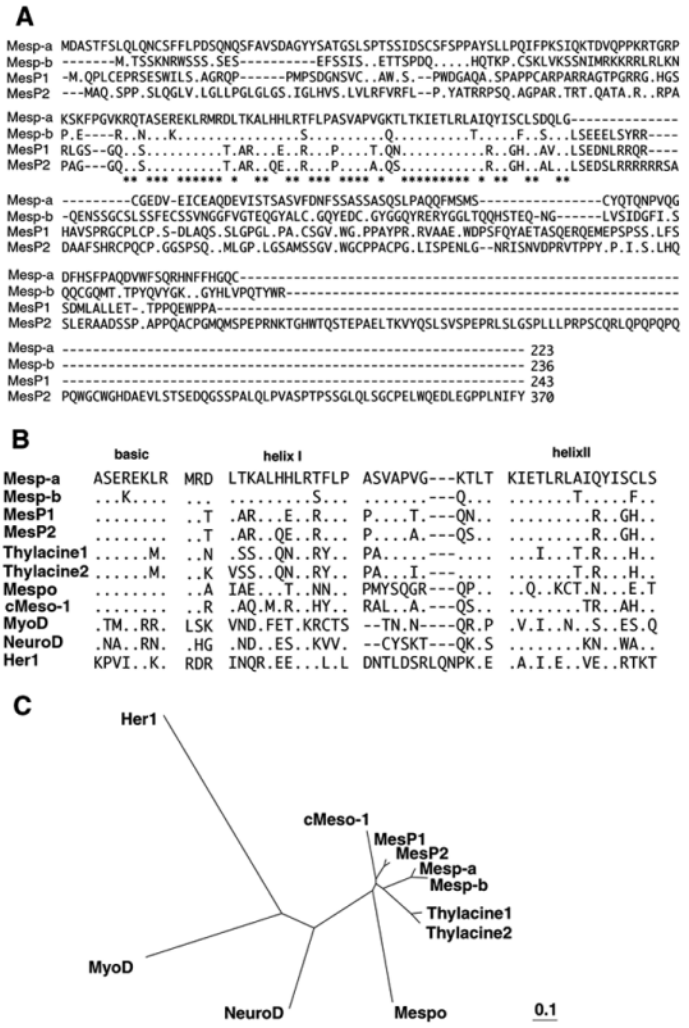

Fig. 1. Sequences of zebrafish Mesp proteins and phylogenetic analysis. (A) Complete peptide sequences of Mesp-a and Mesp-b aligned with murine MesP1 and MesP2. Asterisks under the sequences indicate the position of conserved amino acid. (B) Comparison of Mesp-a and Mesp-b bHLH domains with other members of the bHLH family. Dots indicate identical amino acids. Dashes represent gaps introduced to maximize the alignment. (C) A phylogenetic tree of bHLH transcription factors. The tree is constructed by the NJ method (Saitou and Nei, 1987) using the sequences shown in (B). GenBank accession numbers: *mesp-a*, AB037939; *mesp-b*, AB037940 (*mesp-a* also assigned AF188833).

(46/51), while no homology is seen outside the bHLH domain (Fig. 1A).

A database search with the deduced amino acid sequences revealed several closely related bHLH family members (Fig. 1B). The Mesp-a (Mesp-b) bHLH domain showed 73% (72%), 71% (69%), 55% (57%), 67% (65%), 76% (75%) and 75% (73%) identity to those of Thylacine 1, Thylacine 2 (*Xenopus*; Sparrow et al., 1998), Mespo (*Xenopus*; Joseph and Cassetta, 1999), cMeso-1 (chick; Buchberger et al., 1998), MesP1 and MesP2 (mouse; Saga et al., 1996 and 1997), respectively. In contrast, it is only 47% (45%), 33% (31%) and 31% (28%) identical to zebrafish NeuroD (Blader et al., 1997; Korzh et al., 1998), MyoD (Weinberg et al., 1996) and Her1 (Müller et al.,

1996), respectively (Fig. 1B). Essentially no homology to those or any other proteins was found outside of the bHLH domain at the nucleotide or protein level. Based on this similarity and the phylogenetic tree (Fig. 1C), we concluded that zebrafish *mesp-a* and *mesp-b* belong to the *Mesp*-related subfamily of bHLH transcription factors.

Expression of the zebrafish *mesp-a* and *mesp-b* genes during embryonic development

Whole-mount in situ hybridization with digoxigenin-labeled or fluorescein-labeled probes was performed to investigate the embryonic expression patterns of these two genes. To avoid cross hybridization between the similar bHLH transcripts, we used probes which excluded the bHLH regions. The nucleotide sequences outside the bHLH of *mesp-a* and *mesp-b* differ significantly and the probes used provided distinct expression.

mesp-a transcripts are first seen at 30% epiboly in the blastoderm margin (data not shown). Expression was detected as an homogenous ring around the margin with a small gap (about one-eighth of the ring). This expression pattern was maintained until early gastrula stages (Fig. 2A). Double staining with *mesp-a* and *goosecoid* (Stachel et al., 1993) probes at the shield stage revealed that the most dorsal margin is devoid of *mesp-a* (Fig. 2B). As gastrulation proceeds, the expression at the dorsolateral margin becomes broad along the animal-vegetal axis, while that at the ventral margin declines (Fig. 2C). Histological sections demonstrated that the transcripts were restricted to the hypoblast cells during gastrulation (data not shown). During mid to late gastrulation, dorsolateral expression above the margin becomes narrowed along the dorsal-ventral axis probably due to dorsal convergence movement. Before the end of gastrulation, at about 95% epiboly, a pair of transverse stripes of *mesp-a*-expressing cells separates from the marginal domain (Fig. 2D, see also Fig. 4A-C). In contrast to *mesp-a*, *mesp-b* is not expressed during early to mid gastrulation (Fig. 2G). Expression of *mesp-b* is first seen at the end of gastrulation in stripes in the paraxial mesoderm. Throughout the segmentation period, expression of *mesp-a* and *mesp-b* is detected in stripes of cells located on either side of the neural tube. As segmentation proceeds, the position of the stripes shifted progressively towards the posterior part of embryos by switching off the most rostral stripe near the forming somites and initiating a new expression domain caudal to the most caudal stripe. The expression domain is initially broad but the most anterior stripes are usually narrower. The expression patterns are dynamic and the number of stripes varies between one to three: one to two stripes are most often observed for *mesp-a* while two to three are seen for *mesp-b* (Fig. 2E,F,H,I). Two-colour in situ hybridization with *mesp-a* and *mesp-b* probes demonstrated that both genes are activated at approximately the same time and the same level during the segmentation period (Fig. 2J,K). However, the transcripts of *mesp-b* tend to be more persistent, leaving the most anterior stripe of *mesp-b* located anterior to that of *mesp-a* (Fig. 2I, see also Fig. 3B,C)

Histological sections of stained embryos show that the *mesp* transcripts are in the PSM, posterior to the segmented somites (Fig. 3A). To precisely localize the transcripts within the PSM, we compared the expression patterns of *mesp-a* and *mesp-b*

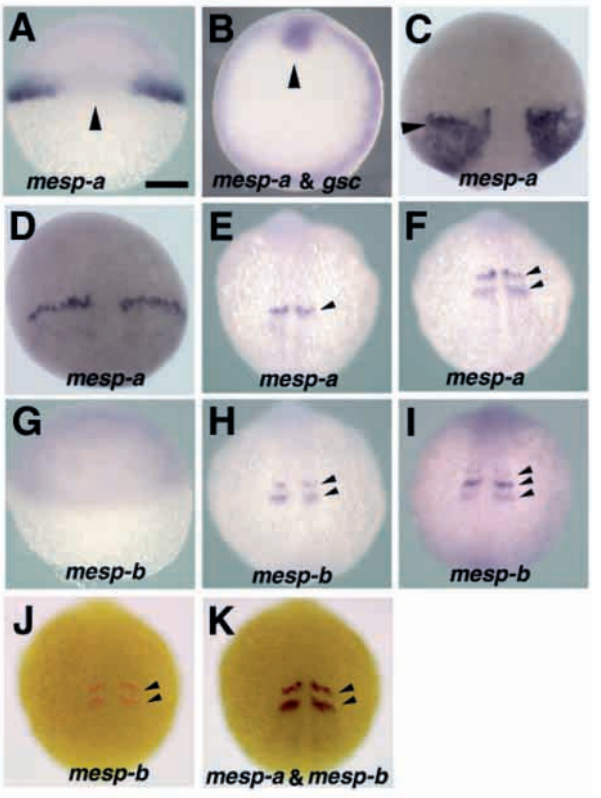

Fig. 2. Normal expression patterns of *mesp-a* and *mesp-b* transcripts in zebrafish embryos. Embryos are oriented with anterior (animal pole) to the top (except for B, in which the embryo is viewed from the animal pole). (A,B) *mesp-a* expression at the shield stage. *mesp-a* is expressed in the blastoderm margin with a small gap (arrowhead, A). (B) Animal-pole view of an embryo double-stained with *goosecoid* (*gsc*). *gsc* expression is seen within the gap in *mesp-a* expression (arrowhead). (C-F) Dorsal views of embryos hybridized with a *mesp-a* probe at 80% epiboly (C), 100% epiboly (D) and 10- to 12-somite stages (E,F). As gastrulation proceeds the marginal expression expands along the animal-vegetal axis in the dorsal region (anterior edge indicated by arrowhead in C). However, the expression is rapidly down-regulated in most of the area except in the anterior border, leaving a pair of stripes (D). During the segmentation period, one or two stripes of expression are visible (arrowheads in E,F). (G-I) *mesp-b* expression at the shield stage (G) and 10- to 12-somite stages (H,I). No *mesp-b* expression is detected during gastrulation. During the segmentation period, two or three stripes of expression are visible (arrowheads in H,I). (J,K) Two-colour staining with DIG-labeled *mesp-a* and fluorescein-labeled *mesp-b* probes at the 10-somite stage. The embryo was first processed for *mesp-b* staining, then photographed (red in J), followed by *mesp-a* staining (blue in K). The expression domains of *mesp-a* and *mesp-b* overlap (arrowheads, K). Bars, 100 μm.

with other known genes expressed in this specific region. We first used the *myoD* expression pattern as a reference. *myoD* is expressed in the posterior parts of somites adjacent to the furrow, and one or two fainter pairs of bands are seen in the posterior parts of the somite just undergoing furrow formation (S0) and more posteriorly in the paraxial mesoderm (Weinberg et al., 1996). Two-colour in situ hybridization shows that, when three bands of *mesp-b* expression are present, they are located posteriorly adjacent to the posterior faint bands of *myoD* (Fig. 3C). It was difficult to determine whether or not any cells

expressed both *myoD* and *mesp* genes. The staining also shows that, unlike *mesp-b*, *mesp-a* expression domain includes the adaxial cells that are located on either side of the notochord and are positive for *myoD* (asterisk in Fig. 3B). We then used *paraxial protocadherin* (*papc*; Yamamoto et al., 1998) to localize *mesp* transcripts within the somite primordia. Zebrafish *papc* is expressed in four bilateral pairs of bands in the paraxial mesoderm during the segmentation period. The first band is located in the anterior border of the newest somite formed (SI) and the second in the forming somite (S0). The two posterior, stronger bands seem to be located in successive somite primordia. Two-colour in situ hybridization shows that the three bands of *mesp-b* are located within the posterior three bands of *papc* and share the same anterior boundary (Fig. 3D,E). Thus, it is likely that the most anterior stripes of *mesp-b* correspond to the anterior of the forming somite (S0) and that the posterior two stripes are in two successive somite primordia. Accordingly, *mesp-a* is expressed in one and/or two primordia posterior to the forming somites. The spatial relationship between *myoD*, *papc* and *mesp* expression is schematically represented in Fig. 3F.

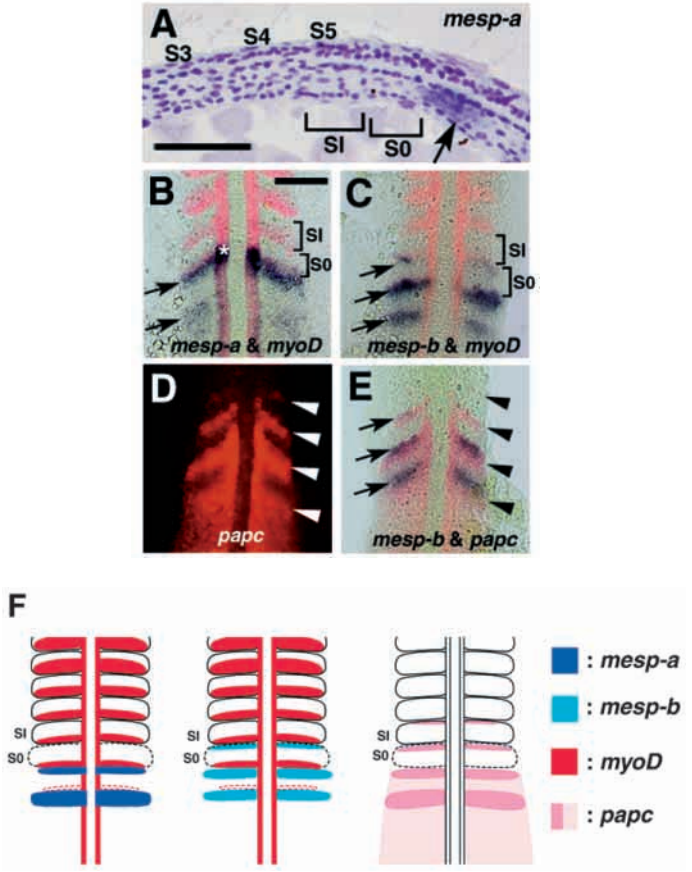

Fig. 3. Expression patterns of *mesp-a* and *mesp-b* in the presomitic mesoderm. Embryos are oriented with anterior to the top (except for A, in which anterior is to the left). (A) Longitudinal section through a 5-somite stage embryo hybridized with a *mesp-a* probe. Somites 3, 4 and 5 are labeled as S3, S4 and S5. A newly formed and forming (or the most anterior presumptive) somites are designated as SI and S0, respectively. The *mesp-a*-positive region (arrow) is located posterior to S0. (B,C) Two-colour staining with *myoD* (red) and *mesp-a* (blue in B) or *mesp-b* (blue in C) at the 10-somite stage. Dorsal views of flat-mounted embryos are shown. Arrows indicate the stripes of *mesp* genes. (D,E) Two-colour staining with *paraxial protocadherin* (*papc*, red) and *mesp-b* (blue) at the 10-somite stage. Dorsal views under fluorescence (D) and bright-field optics (E) are shown. Arrowheads indicate the anterior borders of *papc* expression domains and arrows indicate *mesp-b* expression stripes. Note that both expression domains overlap, sharing the same anterior border. (F) Simplified diagrams illustrating expression patterns of *mesp-a*, *mesp-b*, *myoD* and *papc*. Bars, 50 μm.

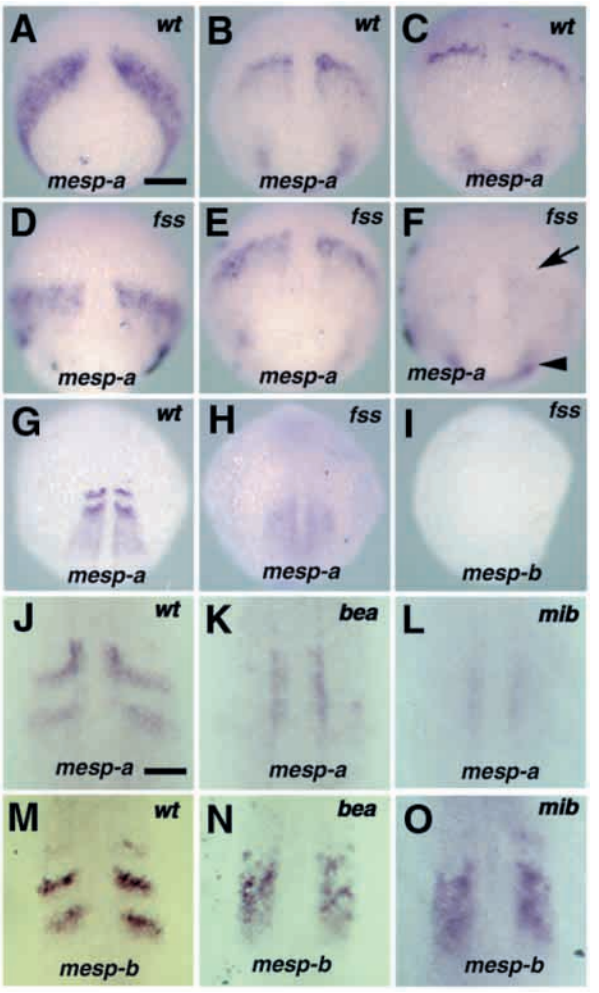

Fig. 4. *mesp* expression in *fss*-type mutants. In all panels, the genotype of embryo is shown in the upper right corner and the probe used is at the bottom. (A-I) *mesp* expression in wild-type and *fss* embryos at 70% epiboly (A,D), 90% epiboly (B,E), 95% epiboly (C,F) and 12-somite stages (G-I). The normal expression pattern of *mesp-a* is seen in both wild-type and *fss* embryos up to 90% epiboly. In *fss* embryos, however, the striped expression is not maintained in later stages (arrow in F) while the expression at the blastoderm margin persists (arrowhead in F). Neither *mesp-a* nor *mesp-b* is expressed in *fss* mutants during segmentation (G-I). *mesp* expression in wild-type (J,M), *bea* (K,N) and *mib* (L,O) embryos at the 10-somite stage. *mesp-b* expression loses its striped pattern and shows a 'salt and pepper' pattern, which covers a region two- to three-somites wide in the paraxial mesoderm (N,O). As compared with *mesp-b*, *mesp-a* expression in the mutants is very weak and diffuse, and sometimes undetectable except for that in the adaxial cells (K,L). Bar in A, 100 μm; in J, 30 μm.

mesp-a and *mesp-b* expression in mutant embryos showing segmentation defects

The expression patterns of the *mesp* genes suggest that they function in the segmentation of the paraxial mesoderm. Given that the *fss*-type genes (van Eeden et al., 1996), identified by mutation, are involved in segmenting the paraxial mesoderm, we examined the expression patterns of *mesp-a* and *mesp-b* in mutants of this group. The mutants of *fss*-type genes, *fss*, *bea*, *des*, *aei* and *mib*, exhibit a defect in somite boundary formation. However, the spatial distribution of the defects is different among mutants: *fss* controls the formation of all somites while the other four only govern the formation of caudal somites, the first several somites remain intact in these mutants.

In *fss* mutants, neither *mesp-a* nor *mesp-b* expression is detected in the PSM throughout the segmentation period (Fig. 4G-I). During gastrulation, by contrast, all *fss* mutants show normal *mesp-a* expression, suggesting that *mesp-a* is upstream of *fss* or in a different pathway, at least during gastrulation. However, the expression in the paraxial mesoderm disappears in the mutant at 95% epiboly (arrow in Fig. 4F) when in wild-type embryos the rostral expression domain become restricted to a pair of narrow stripes (Fig. 4A-F). The marginal expression of *mesp-a* still persists at this stage (arrowhead in Fig. 4F)

In the other four mutants, *bea*, *des*, *aei* and *mib*, the transcripts of both *mesp-a* and *mesp-b* are detected but their intensity is highly variable. In all these mutants, the *mesp-b* expression pattern is no longer striped but shows a mosaic 'salt and pepper' pattern, which covers a region two- to three-somites wide in the paraxial mesoderm (Fig. 4M-O). As compared with *mesp-b*, *mesp-a* expression in these mutants tend to be very weak and diffuse, and sometimes undetectable except for that in the adaxial cells (Fig. 4J-L).

Overexpression of Mesp-b affects the anteroposterior specification within the somites, leading to a segmentation defect

To study the roles of zebrafish Mesp-a and Mesp-b in somitogenesis, we overexpressed these proteins by injecting capped RNA into one-cell stage zebrafish embryos. Overexpression of Mesp-a caused a severe gastrulation defect, probably due to the inhibition of mesoderm formation (data not shown). In contrast, overexpression of Mesp-b showed specific effects on somitogenesis. Thus, we concentrated on the functional analysis of Mesp-b. RNA encoding β-galactosidase was coinjected with the RNA to be overexpressed to localize the injected RNAs. Control injections using *green fluorescent*

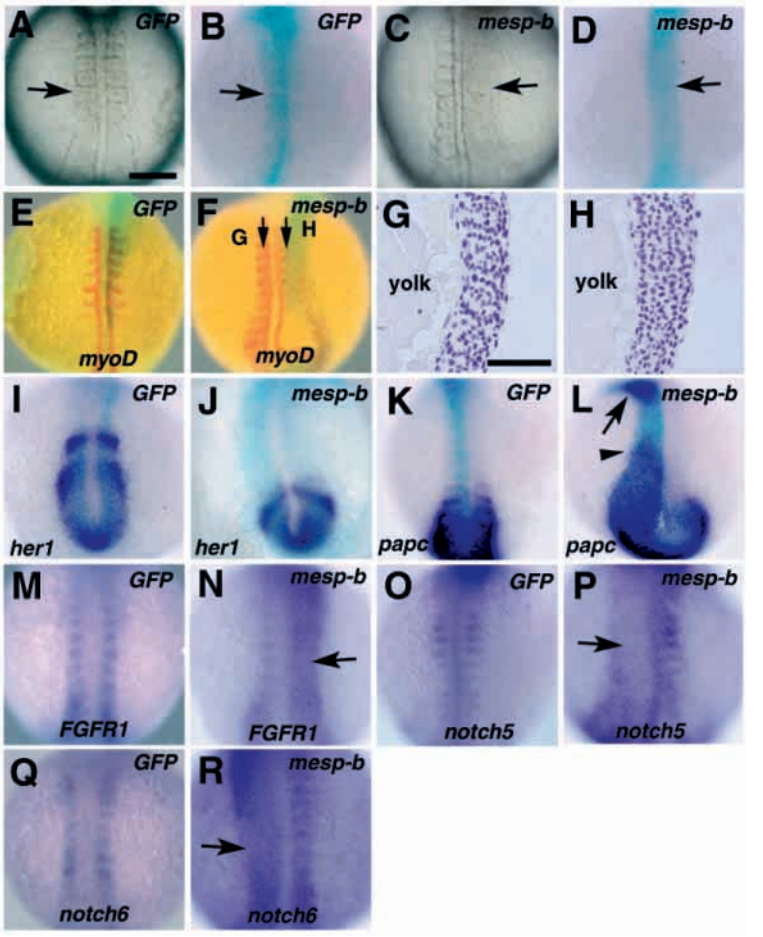

Fig. 5. Effect of Mesp-b misexpression on somite formation. Whole-mount samples are viewed dorsally. In all pictures, embryos at the 8- to 12-somite stages are shown and oriented with anterior to the top. The injected RNA is noted in the upper right corner and the probe used is at the bottom. Light blue staining in B,D-F and I-L marks the localization of coinjected β-galactosidase. The samples in M-R were not stained for β-galactosidase activity, which sometimes affects weak in situ staining. The injected embryos showing severe segmentation defects were selected and processed for *notch* or *FGFR1* staining. (A-D) Live embryos injected with *GFP* (A) or *mesp-b* (C) and β-galactosidase staining of the same embryos (B,D). Somites fail to form in the *mesp-b*-injected region (arrow in C,D). (E-H) *GFP* RNA injection does not affect *myoD* expression (red staining, E), while segmental *myoD* expression is either lost or disrupted by the overexpression of *mesp-b* (F). (G,H) Longitudinal sections of the sample at the levels indicated by the arrows in F. Segmentation is disturbed only in the injected region (H). (I,J) *her1* expression in *GFP*-injected (I) and *mesp-b*-injected (J) embryos. In the *mesp-b*-injected embryo (J), light blue staining for β-galactosidase activity is seen on both sides of the embryos. Although *her1* expression domains become irregularly shaped, *mesp-b* injection does not affect the segmental expression of *her1*. (K,L) *papc* (blue) expression in *GFP*-injected (K) and *mesp-b*-injected (L) embryos. *papc* loses its segmental expression in the anterior presomitic mesoderm following *mesp-b* injection. In some cases, *papc* expression is not down-regulated correctly, resulting in the anteriorly expanded expression (arrowhead in L). Furthermore, expression of *papc* is sometimes elevated in the head mesenchyme (arrow in L). (M,N) *FGFR1* expression in *GFP*-injected (M) and *mesp-b*-injected (N) embryos. The expression, which is normally restricted to the presomitic mesoderm and the anterior of formed somites, loses its segmental pattern in the *mesp-b*-injected region (arrow in N). (O,P) *notch5* expression in *GFP*-injected (N) and *mesp-b*-injected (O) embryos. The expression, which is normally restricted to the posterior of formed somites (O), is down-regulated in the *mesp-b*-injected region (arrow in P). (Q, R) *notch6* expression in *GFP*-injected (Q) and *mesp-b*-injected (R) embryos. The expression, which is normally restricted to the anterior of formed somites, loses its segmental pattern in the *mesp-b*-injected region (arrow in R). Bars in A and G, 100 and 50 μm respectively.

protein (GFP) RNA did not cause any disturbance of somitogenesis or gene expression (Fig. 5A,B).

With the injection of an appropriate amount of *mesp-b* RNAs (40-50 pg), a disturbance of segmentation was frequently seen (Fig. 5C,D). The severity of this phenotype varied, ranging from the most severe in which many somites failed to form (125/160), to a less severe one where a region of the somites were irregularly formed (11/160). However, we found a close correlation between defects and the presence of the injected RNAs (22/22; Fig. 5C,D,H). Histological sections revealed that, in the affected region, segmentation is severely affected, but no sign of tissue damage such as cell death was observed (Fig. 5G,H).

We then determined whether overexpression of Mesp-b affected the expression of several genes implicated in somitogenesis. Expression patterns of *her1*, *myoD*, *papc*, *FGFR1*, *notch5* and *notch6* were examined in injected embryos in which defects in boundary formation were clearly visible at the 8- to 12-somite stage. The severity and number of embryos affected varied between different experiments, depending on the distribution of the injected RNAs. Representative embryos are shown in Fig. 5E,F,I-R.

In control embryos of the 8- to 12-somite stage, *her1* is expressed in two or three stripes in the PSM and *papc* in three to four stripes near and over the point of somite formation. In injected embryos, the length of the PSM (the distance between the tailbud to forming somites) tended to be shorter, but the segmental expression of *her1* persisted in the injected region that was positive for β-galactosidase activity (6/8; Fig. 5I,J). In contrast, ectopic expression of Mesp-b caused a uniform expression of *papc* in the PSM (10/12; Fig. 5K,L). In some cases, the anterior boundary of the *papc* expression was shifted anteriorly as compared to the uninjected region (arrowhead in Fig. 5L). Furthermore, *papc* expression was increased in the head mesenchyme (arrow in Fig. 5L). *myoD* expression was almost lost in regions where Mesp-b was overexpressed (10/10; Fig. 5E,F).

Since *papc* is expressed in the anterior parts and *myoD* in the posterior parts of forming and segmented somites, the above results suggest that development of posterior fate within the somites is suppressed in the Mesp-b-injected region. To further verify this idea, we examined the expression pattern of *FGFR1*. In control embryos, *FGFR1* expression is detected uniformly throughout the PSM but after somite formation the expression in a posterior domain of each somite is down-regulated, resulting in a segmented pattern in the somitic region (Fig. 5M; a manuscript on *FGFR1* expression pattern is in preparation by K. Y.). This expression pattern is similar to that described for the mouse orthologue (Orr-Urtreger et al., 1991; Yamaguchi et al., 1992). As shown in Fig. 5N (arrow), injected embryos had a disrupted pattern of *FGFR1* expression; on the injected side, *FGFR1* was not down-regulated in the somitic region, instead it was uniformly expressed throughout the paraxial mesoderm (8/8).

To further examine the effect on the anteroposterior specification within the somites, we looked at the expression of *notch5* and *notch6* which are segmentally expressed in the anterior PSM and/or formed somites (the probes used were derived from PCR-amplified fragments based on the sequences of notch5 and notch6; Westin and Lardelli, 1997). Transcripts of *notch5* are detected in the posterior parts of presumptive and formed somites (Fig. 5O), while *notch6* is expressed in the PSM and the anterior parts of somites (Fig. 5Q), in a complementary pattern to *myoD* expression (Westin and Lardelli, 1997). Although their expression is weak, consistent results were obtained in injected embryos: ectopic expression of Mesp-b significantly down-regulated *notch5* (6/6; Fig. 5P), whereas it up-regulated *notch6* in the gaps which resulted in uniform expression in the paraxial mesoderm (8/8; Fig. 5R).

All these results support the idea that overexpression of Mesp-b enhances the anterior fate of somites at the expense of posterior one.

Relationship between *mesp-a* and *her1* expression

mesp-a expression is first detected in the blastoderm margin but stripes of expression become apparent in the paraxial

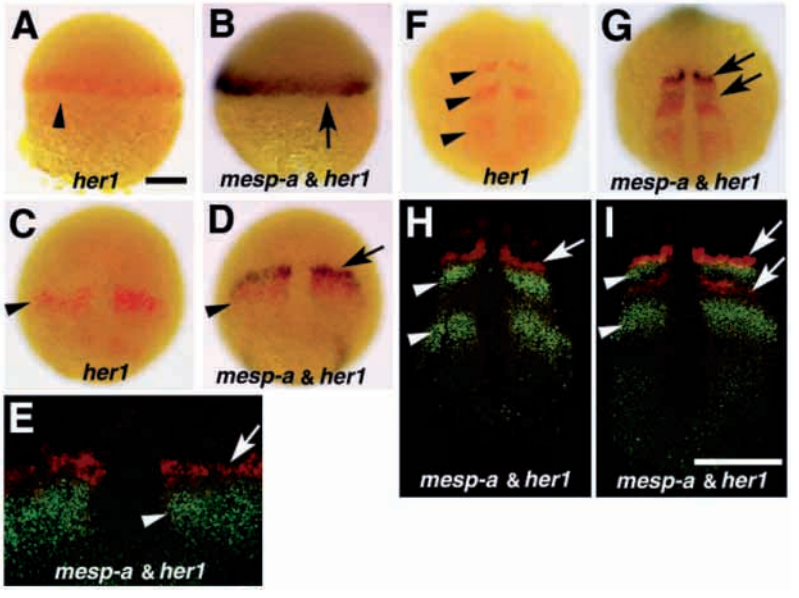

Fig. 6. Relationship between *mesp-a* and *her1* expression domains from gastrula to early segmentation period. In all pictures, the probe used is shown at the bottom. Two-colour staining with *mesp-a* and *her1* at shield (A,B), 90% epiboly (C-E) and 5-somite (F-I) stages. Lateral views with dorsal to the right (A,B) and dorsal views with anterior to the top (C-I) are shown. Arrowheads indicate *her1* expression domains and arrows indicate *mesp-a*. Hybridized embryos were first processed for *her1* (red) staining, photographed, and then processed for *mesp-a* (blue) staining (A-D,F,G). In E,H and I, hybridized signals were visualized with Fast Red and ELF-97 (see Material and Methods), and the flat-mounted samples were viewed under fluorescent microscopy (*mesp-a* in red and *her1* in green). At the shield stage, the expression domain of *mesp-a* overlaps with that of *her1* (A,B). As gastrulation proceeds, they become completely segregated such that the *mesp-a* stripes are located more anteriorly (arrow and arrowhead in D and E). During the segmentation period, the anteriormost decaying stripes of the two genes are partially overlapped, while the stripes are seen juxtaposed at the stage when the only one pair of *mesp-a* strip is observed (F-I). Bars, 100 μm.

mesoderm during the late gastrulation period (Fig. 2C-D). This early expression pattern is reminiscent of that of *her1*, a zebrafish bHLH gene related to the *Drosophila* pair-rule gene *hairy* (Müller et al., 1996). *her1* is expressed in the blastoderm margin and in two distinct transverse bands of hypoblastic cells above the margin. After the completion of epiboly, this pattern remains essentially unchanged throughout the segmentation period. Lineage tracing experiments have demonstrated that the cells in the *her1* expression domain I (the first stripe) are incorporated into the 5th somite (Müller et al., 1996).

To determine the relationship between *mesp-a* and *her1*, we analyzed their relative expression patterns in embryos of mid-gastrula to early segmentation stage by two-colour in situ hybridization. In these experiments, the embryos hybridized with *her1* and *mesp-a* probes were first stained for *her1* in red, then photographed. This was followed by visualization of *mesp-a* transcripts in blue (Fig. 6A-D,F,G). As shown in Fig. 6A and B, the expression domains of *mesp-a* and *her1* in the marginal region initially overlap at the shield stage. At mid- to late gastrula stages, the anterior expression bands for both genes are separated from the marginal expression domain, and they are segregated such that *mesp-a* expression is located anteriorly to *her1* (domain I) (Fig. 6C,D). Double fluorescent in situ hybridization with *mesp-a* (red) and *her1* (green) show that the expression domains of each gene are completely segregated, although they are juxtaposed to each other (Fig. 6E). These results, together with the lineage tracing experiments of *her1*-expressing cells (Müller et al., 1996), suggest that the precursors for the first three to four somites do not express *mesp-a*.

During the segmentation period, the anteriormost stripes of *mesp-a* and *her1* are seen juxtaposed or partially overlapped. There is a tendency for the overlapping region to be observed when two pairs of *mesp-a* stripes are detected, but not when the only one pair of *mesp-a* stripes is detected (Fig. 6F-I). These two staining patterns were reproducibly obtained at all segmentation stages examined. However, this result appeared contradictory to that reported by Müller et al (1996) because, in the trunk region, *her1* expression has been proposed to follow a pair-rule pattern in alternating somite primordia, whereas *mesp* expression is detected in all somite primodium. Thus, we re-examined *her1* expression using *mesp-a* expression as a reference. We collected embryos between 5- to 7-somite stages and re-staged them according to the following morphological criteria before fixing. Each stage was further divided into three sub-stages: the n-somite stage when boundary formation is just completed, the n-somite+ stage when the presomitic cells that will contribute to the future next somite become aggregated and the next furrow formation has started, and the n-somite++ stage when furrow formation has proceeded to half way. These morphological criteria were determined by a lateral view of a live embryo. It should be noted that we are not able to judge accurately the lengths of individual stages. Arranging a series of pictures in order, we noticed that *her1* expression domains move in a caudal to rostral direction although the posterior tip of the tailbud is

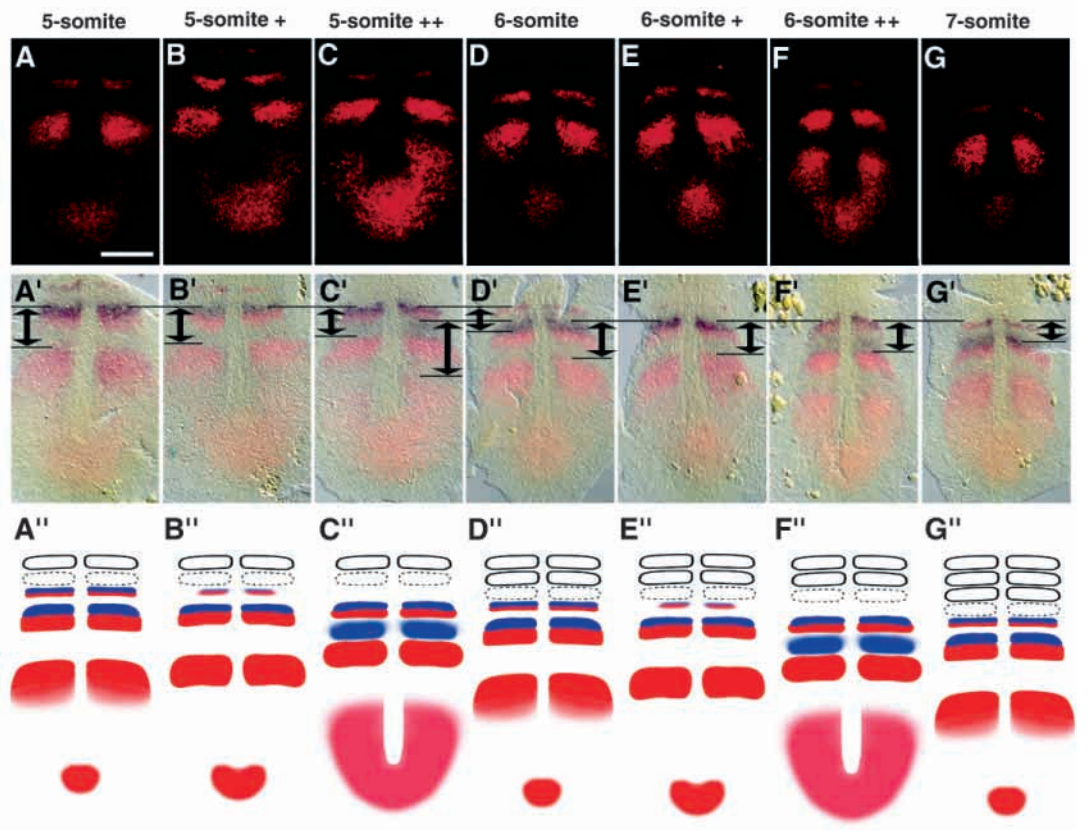

Fig. 7. Temporal and spatial cycle of *her1* expression in the presomitic mesoderm between 5- and 7-somite stages. For staging criteria, see text. The embryos which had been hybridized with *her1* and *mesp-a* probes were first processed for *her1* staining (Fast Red), followed by *mesp-a* staining (BM purple). A pair of photographs in upper (A-G; rhodamine filter) and lower (A′-G′; bright field) panels were taken of the same flat-mounted samples. Under the rhodamine filter, only the *her1* signal is sensitively detected. Simplified diagrams illustrating expression profile of *her1* (red) and *mesp-a* (blue) are shown at the bottom (A″-G″). Solid lines represent formed somites while dotted lines represent successively forming somites. The *her1* expression domain appears around the tailbud, and moves anteriorly until it finally overlaps with the most anterior stripe of *mesp-a*. Both stripes disappear near the point of furrow formation. The posterior tip of the tailbud is always positive for *her1* transcripts. A stripe of *her1* appears every 30 minutes in the tailbud region, and persists for about 1.5 hours (three somite cycles in zebrafish). Since we cannot judge accurately the lengths of individual sub-stages, we make no claim that the diagrams at the bottom are evenly spaced in time. Bars, 100 μm.

always express *her1* transcripts (Fig. 7A-G,A′-G′). We examined seven independent series of embryo collections and all results were consistent. The *her1* stripes, which appear in the tailbud region, become narrower as they migrate, and finally overlap the most rostral decaying *mesp* stripes before both transcripts disappear (Fig. 7). A wave leaves the tailbud region every 30 minutes and takes 1.5 hours to complete one cycle and to disappear. Thus, all somite primordia (except for the first few) become positive for *her1* and *mesp-a* prior to segmentation.

DISCUSSION

Mesp family of bHLH transcription factors expressed in the newly formed mesoderm and the rostral PSM

In this study, we have isolated two zebrafish cDNAs that encode bHLH transcription factors related to murine MesP1 and MesP2. Recently, *Mesp*-related genes have been isolated in *Xenopus* (*Thylacine*, Sparrow et al., 1998; *Mespo*; Joseph and Cassetta, 1999) and chick (*cMeso-1*, Buchberger et al., 1998). Their bHLH domains are highly homologous to each other, forming a novel family of bHLH transcription factors that we refer to as the Mesp family. Outside the bHLH region, however, essentially no homology can be found among Mesp family proteins. Based on the phylogenetic tree (Fig. 1C), it is likely that the independent duplication of the *mesp* gene occurred in each vertebrate during evolution. In spite of this, the expression pattern and genomic organization of murine *Mesp1* and *Mesp2* are very similar to those of zebrafish *mesp-a* and *mesp-b*. *mesp-a* and *mesp-b* have a nearly identical expression pattern to murine *Mesp1* and *Mesp2*, respectively. Only *Mesp1* and *mesp-a* are expressed in the early mesoderm (the primitive streak and the blastoderm margin), while the expression in the PSM is almost the same for all four genes, albeit the number of expression stripes varies. Although the precise genomic organization of *mesp-a* and *mesp-b* is not clear yet, our mapping data (see below) and the fact that *mesp-b* was isolated from a PAC clone containing *mesp-a* suggest that the two genes are located within a region of less than a few hundred kb. Similarly, *Mesp1* and *Mesp2* are located in chromosome 7, head to head, and separated by 23 kb (Saga et al., 1997).

Presomitic segmental pattern and an anteroposterior polarity within presumptive somites

All identified Mesp family members are expressed in a subdomain of the PSM, immediately posterior to the forming somites (Saga et al., 1996 and 1997; Sparrow et al., 1998; Buchberger et al., 1998; Joseph and Cassetta, 1999). In addition to the Mesp family, other bHLH transcription factors, such as zebrafish *her1*, chick *c-hairy1*, and *Xenopus Hairy2A* (Jen et al., 1997), are segmentally and/or transiently expressed in the PSM, suggesting that the bHLH family play an important role in establishing a segmental prepattern prior to somitogenesis. Interestingly, some of them show a preferential expression within prospective anterior or posterior parts of somites, suggesting they have roles in anteroposterior specification of the somite primordia. *Thylacine* expression is restricted to the anterior halves of the somitomeres while *Hairy2A* is in the posterior halves. Similarly, this study revealed that at least the most rostral expression domain of zebrafish *mesp-a* and *mesp-b* resides in the anterior part of the future somite. Although the expression stripes of murine *Mesp* genes and chick *cMeso-1* are approximately one somite wide, the analysis of *lacZ* expression driven by *Mesp2* promoter suggests that the cells that have expressed *Mesp2* mainly contribute to the anterior parts of the mature somites (data not shown). These facts strongly support the existence of a segmental prepattern and an anteroposterior polarity in the PSM, in agreement with the results of experimental manipulations performed in several organisms (Keynes and Stern, 1988; Elsdale et al, 1976; Cooke, 1978; Kimmel et al., 1988; Primmett et al., 1988; Roy et al., 1999).

The first stripe of *mesp-a* expression domain seems to demarcate the area of the future 5th-somite level during gastrulation

The *mesp-a* expression domain at the blastoderm margin contains all the cells that will involute, or ingress, to form mesoderm derivatives (Kimmel et al., 1995). During involution and dorsal convergent movement, *mesp-a*-positive cells are mainly located in the future paraxial mesoderm. However, the expression soon disappears in the paraxial mesoderm except for the most rostral region, leaving a pair of stripes in the PSM. A similar dynamic expression pattern has been reported for zebrafish *her1*. Two-colour in situ hybridization analysis demonstrates that the expression domains of *mesp-a* and *her1* initially overlap but that they are soon segregated during late gastrulation when their striped expression patterns become apparent. *mesp-a* stripes are always located just anterior to those of *her1* (Fig. 6E). This relationship is maintained until the onset of segmentation.

Since lineage-tracing analysis demonstrated that the first pair of *her1* stripes (domain I) resides in a primordium of the future 5th somite (Müller et al., 1996), neither *mesp-a* nor *her1* is expressed in the cells that contribute to the first several somites (maybe four). These results suggest the existence of distinct mechanisms for rostral and caudal segmentation. In addition, as reviewed by Jiang et al. (1998), several other observations further strengthen this idea. First, the earliest few somites in zebrafish seem to form more quickly than later ones: 3 per hour for the first six, and 2 per hour thereafter (Kimmel et al., 1995). Secondly, in *fss*-type mutants except for *fss*, segmentation defects are visible only in the region posterior to the 4th to 8th somite level (van Eeden et al., 1996). Thirdly, several early somites in the cervical region are generated in *Wnt3a*- and *Mesp2*-deficient mice in which segmentation in the trunk and tail regions is severely impaired (Takada et al., 1994 and Saga et al., 1997).

Holland et al. (1997) found that a homologue of the *engrailed* gene is expressed only in the first eight somites of amphioxus. In amphioxus embryos the first eight somites are formed by a primitive mechanism by which epithelial outpockets are pinched off the primitive gut, whereas more caudal somites are formed by a common vertebrate mechanisms by which mesenchymal cell sheets are subdivided into segments. In spite of differences in the mode of segment formation in amphioxus and in higher vertebrates, several schemes for aligning the segments in amphioxus and vertebrates have been proposed. For example, the sixth somite

of amphioxus is equated to the sixth somite in the lamprey and shark and to the first true somites in the chick (Gilland and Baker, 1993). All these observations suggest the presence of a distinct mechanism for the rostral segmentation. Therefore, it will be of interest to clone Mesp family members from amphioxus and to determine their anterior expression boundary.

Waves of *her1* expression in the PSM

Using the *mesp-a* expression pattern as a reference, we found that zebrafish *her1* transcripts oscillate in the PSM with a regular periodicity before decaying near the point of segmentation. In the trunk region, *her1* expression overlaps with the anterior *mesp-a* expression domain and, consequently, every somite primordium is positive for *her1* transcripts prior to segmentation. This dynamic expression pattern is highly reminiscent of that reported for *c-hairy1* which provided the first molecular evidence for an intrinsic clock linked to somite segmentation (Palmeirim et al., 1997). The expression of *c-hairy1* appears as a wave, which sweeps across the PSM once during each somite formation, and stabilizes in the posterior half of the next budding somite. Although zebrafish *her1* is not maintained in the somite, it is likely that the cycling behavior of *hairy*-related genes is conserved among vertebrates. The wave of *c-hairy* does not result from cell displacement or from signal propagation in the PSM but rather reflects an intrinsically coordinated clock which do not require protein synthesis (Palmeirim et al., 1997). The nature of the *her1* wave in zebrafish should also be examined in this context.

Zebrafish Mesp-a and Mesp-b are downstream targets of *fss* during the segmentation period but differentially regulated by other *fss*-type genes

During the segmentation period, expression of *mesp-a* and *mesp-b* in the PSM is completely abolished by the *fss* mutation, indicating that they are downstream targets of *fss*. However, the phenotype of *fss* mutant is not likely to be due to a mutation in a *mesp* gene because mapping of *mesp* genes with a radiation hybrid panel (kindly provided by Dr M. Ekker) showed that zebrafish *mesp* genes are located in LG 7 to which no *fss*-type genes have been mapped so far (Dr Scott Holley, personal communication).

In *fss* mutants, *mesp-a* expression remains normal up to late gastrulation but its rostral expression becomes weak between 90% and 95% epiboly and finally disappears by 100% epiboly. This indicates that *fss* is required for *mesp* expression only in the rostral PSM, suggesting that *fss* functions near the point of segmentation (Fig. 8A). Consistent with this, van Eeden et al. (1998) have reported that the *fss* mutation only affects the most rostral stripes of *her1*: the establishment of a segmental expression pattern is normal in *fss* mutants, but *her1* expression is switched off prematurely in the rostral PSM, resulting in a reduction of number of visible stripes.

In contrast to *fss*, other *fss*-type mutants, *bea*, *des*, *aei* and *mib*, show a weaker effect, and differentially affect *mesp-a* or *mesp-b* expression. The expression of *mesp-a* in the PSM is very weak in these mutants, while the level of *mesp-b* expression is more or less unaffected but its striped expression pattern is lost, probably due to an effect secondary to the irregular segmentation. Thus, in spite of similar expression patterns during the segmentation period, the expression of

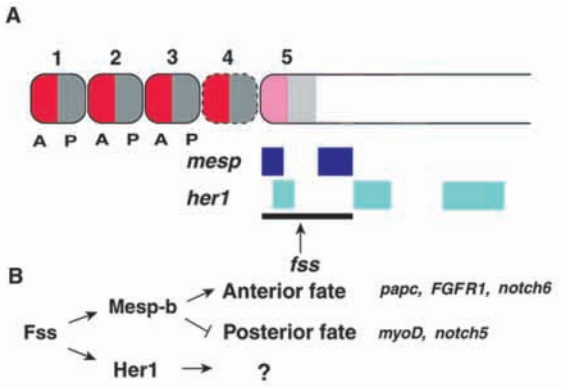

Fig. 8. Schematic presentation of *mesp* and *her1* expression (A) and the proposed activities of Mesp-b (B) in the presomitic mesoderm. Anterior is to the left. The cells that contribute to the first several somites (maybe four) do not express either of the two genes. The gene expression pattern in the presomitic mesoderm demonstrates a molecular prepattern in somitogenesis, i.e., a segmental prepattern in the presomitic mesoderm and the anteroposterior polarity within the presumptive somites (pink and gray). *fss* controls all *mesp* expression and the most rostral expression of *her1* in the presomitic mesoderm. *mesp-b*, which is positively regulated by *fss*, up-regulates the genes that will be expressed in the anterior of the segments (*papc*, *FGFR1*, *notch6*) while down-regulating those in the posterior (*myoD* and *notch5*).

mesp-a and *mesp-b* seems to be differentially regulated. Furthermore, no mutual dependency in their expression has been observed so far. Misexpression of Mesp-b did not affect *mesp-a* expression (data not shown) and, in *Mesp1*- or *Mesp2*-knockout mice, the expression of the intact *Mesp* gene is unaffected (Saga et al., 1997, Saga, 1998).

Mesp-b confers anterior properties on the developing somites

The results obtained by misexpression experiments demonstrate that Mesp-b expressed in the anterior parts of the presumptive and forming somites confers anterior properties on the somite cells. Misexpression of Mesp-b in the normal embryos led to a loss or incorrect formation of somite boundaries. In the injected region, *papc* and *FGFR1* expression, which demarcate the anterior domain of presumptive and/or segmented somites, lost their metameric pattern. In contrast, *myoD* expression in the posterior domain of the somites was greatly reduced. Accordingly, *notch5* expression which would normally be detected in the posterior parts was reduced, while *notch6* expression domain in the anterior parts of the presumptive and segmented somites was expanded, eliminating the gaps in the striped expression pattern. All these data demonstrate that misexpression of Mesp-b expands the anterior character at the expense of the posterior one within both presumptive and segmented somites. Recently a number of studies have shown that FGF-mediated signalling (Deng et al., 1994; Yamaguchi et al., 1994) and Notch-Delta signalling (Conlon et al., 1995; Jen et al., 1997, 1999) are involved in boundary formation. In this study, the expression of the genes involved in these signalling pathways is altered by misexpression of Mesp-b. Together with the fact that the expression of *Notch1*, *Notch2* and *FGFR1* are greatly downregulated in *Mesp2*-deficient mice (Saga et al., 1997), it

is likely that the functions of MesP2 and Mesp-b are mediated via Notch-Delta and FGFR signalling systems.

The defects in boundary formation caused by misexpression of Mesp-b are reminiscent of those reported in *Mesp2*-deficient mice (Saga et al., 1997). Conversely, in this case, the anterior somite fate is suppressed, and the entire somite is posteriorized in identity. Thus, the conclusion drawn from the present gain-of-function experiment is consistent with that from the loss-of-function in *Mesp2*-deficient mice. Severe attenuation of somitogenesis has also been reported in *Xenopus* embryos injected with *Thylacine* RNA and in chick embryos treated with antisense RNA or oligonucleotides of *cMeso-1* (Sparrow et al., 1998; Buchberger et al., 1998), suggesting that the Mesp family genes have a conserved function in vertebrate segmentation.

Taken together, the Mesp family of bHLH transcription factors may act at the same point in vertebrate segmentation, the establishment of anteroposterior polarity within the somite primordia, probably through interacting with the FGFR and the Notch-Delta signalling pathways (Fig. 8B).

We thank Drs Adam Rodaway (King's College London) and Trevor Jowett (University of Newcastle) for their critical comments on β-galactosidase staining and two-colour in situ hybridization, and Mr Hiroshi Onodera for help in isolating zebrafish *FGFR1*. We also thank Drs Charles B. Kimmel (University of Oregon), Sharon L. Amacher (University of California, Berkeley) and Julian Lewis (Imperial Cancer Research Fund) for critical reading of the manuscript. This work was supported in part by CREST (Core Research for Evolutionary Science and Technology) of Japan Science and Technology Corporation (JST), by Bio-Design Project (BDV-00-IV-1-1) and Pioneering Research Project in Biotechnology from the Ministry of Agriculture, Forestry and Fisheries of Japan, and by grants-in-aids from the Ministry of Education, Science, and Culture of Japan. Y.-J. J. would like to thank Dr Julian Lewis for support and was funded by an EMBO long-term fellowship (ALTF 225-1996).

REFERENCES

Amacher S. L. and Kimmel C. B. (1998). Promoting notochord fate and repressing muscle development in zebrafish axial mesoderm. *Development* **125**, 1397-1406.

Aoyama, H. and Asamoto, K. (1988). Determination of somite cells: independence of cell differentiation and morphogenesis. *Development* **104**, 15-28.

Aulehla, A. and Johnson, R. L. (1999). Dynamic expression of *lunatic fringe* suggests a link between *notch* signaling and an autonomous cellular oscillator driving somitic segmentation. *Dev. Biol.* **207**, 49-61.

del Barco Barrantes, I., Elia, A. J., Wünsch, K., Hrabe De Angelis, M., Mak, T. W., Rossant, J., Conlon, R. A., Grossler, A. and de la Pompa, J. L. (1999). Interaction between Notch singalling and Lunatic fringe during somite boundary formation in the mouse. *Curr. Biol.* **9**, 470-480.

Blader, P., Fischer, N., Gradwohl, G., Guillemont, F. and Strähle, U. (1997). The activity of Neurogenin1 is controlled by local cues in the zebrafish embryo. *Development* **124**, 4557-4569.

Buchberger, A., Seidl, K., Klein, C., Eberhardt, H. and Arnold, H. H. (1998). cMeso-1, a novel bHLH transcription factor, is involved in somite formation in chicken embryos. *Dev. Biol.* **199**, 201-215.

Chomczynski, P. and Sacchi, N. (1987). Single-step method of RNA isolation by acid guanidinium thiocyanate- phenol-chloroform extraction. *Analyt. Biochem.* **162**, 156-159.

Christ, B. and Ordahl, C. P. (1995). Early stages of chick somite development. *Anat. Embryol. Berl.* **191**, 381-396.

Conlon, R. A., Reaume, A. G. and Rossant, J. (1995). *Notch1* is required for the coordinate segmentation of somites. *Development* **121**, 1533-1545.

Cooke, J. (1978). Somite abnormalities caused by short heat shocks to pre-neurula stages of *Xenopus laevis*. *J. Embryol. Exp. Morphol.* **45**, 283-294.

Currie, P. D. and Ingham, P. W. (1998). The generation and interpretation of positional information within the vertebrate myotome. *Mech. Dev.* **73**, 3-21.

Deng, C. X., Wynshaw-Boris, A., Shen, M. M., Daugherty, C., Ornitz, D. M. and Leder, P. (1994). Murine FGFR-1 is required for early postimplantation growth and axial organization. *Genes Dev.* **8**, 3045-3057.

Durbin, L., Brennan, C., Shiomi, K., Cooke, J., Barrios, A., Shanmugalingam, S., Guthrie, B., Lindberg, R. and Holder, N. (1998). Eph signaling is required for segmentation and differentiation of the somites. *Genes Dev.* **12**, 3096-3109.

Elsdale, T., Pearson, M. and Whitehead, M. (1976). Abnormalities in somite segmentation following heat shock to *Xenopus* embryos. *J. Embryol. Exp. Morphol.* **35**, 625-635.

Evrard, Y., Lun, Y. Aulehla, A., Gan, L. and Johnson, R. L. (1998). *Lunatic fringe* is an essential mediator of somite segmentation and patterning. *Nature* **394**, 377-381.

Forsberg, H., Crozet, F. and Brown, N. A. (1998). Waves of mouse *Lunatic fringe* expression, in four-hour cycles at two-hour interavals, precede somite boundary formation. *Curr. Biol.* **8**, 1027-1030.

Gilland, E. and Baker, R. (1993). Conservation of neuroepithelial and mesodermal segments in the embryonic vertebrate head. *Acta Anat.* **148**, 110-123.

Halpern, M. E., Hatta, K., Amacher, S. L., Talbot, W. S., Yan, Y. L., Thisse, B., Thisse, C., Postlethwait, J. H. and Kimmel, C. B. (1997). Genetic interactions in zebrafish midline development. *Dev. Biol.* **187**, 154-170.

Holland, L. Z., Kene, M., Williams, N. A. and Holland, N. D. (1997). Sequence and embryonic expression of the amphioxus *engrailed* gene (*AmphiEn*): the metameric pattern of transcription resembles that of its segment-polarity homolog in *Drosophila*. *Development* **124**, 1723-1732.

Hrabe de Angelis, M., McIntyre II, J., and Gossler, A. (1997). Maintenance of somite borders in mice requires the *Delta* homologue *DII1*. *Nature* **386**, 717-721.

Jen, W.-C., Gawantka, V., Pollet, N., Niehrs, C. and Kintner, C. (1999). Periodic repression of Notch pathway genes governs the segmentation of *Xenopus* embryos. *Genes Dev.* **13**, 1486-1499.

Jen, W. C., Wettstein, D., Turner, D., Chitnis, A. and Kintner, C. (1997). The Notch ligand, X-Delta-2, mediates segmentation of the paraxial mesoderm in *Xenopus* embryos. *Development* **124**, 1169-1178.

Jiang, Y. J., Smithers, L. and Lewis, J. (1998). The clock is linked to notch signalling. *Curr. Biol.* **8**, R868-871.

Joseph, E. M. and Cassetta, L. A. (1999). *Mespo*: a novel basic helix-loop-helix gene expressed in the presomitic mesoderm and posterior tailbud of *Xenopus* embryo. *Mech. Dev.* **82**, 191-194.

Jowett, T. and Yan, Y.-L. (1996). Double fluorescent in situ hybridization to zebrafish embryo. *Trends Genet*. **12**, 387-389.

Keynes, R. J. and Stern, C. D. (1984). Segmentation in the vertebrate nervous system. *Nature* **310**, 786-9.

Keynes, R. J. and Stern, C. D. (1988). Mechanisms of vertebrate segmentation. *Development* **103**, 413-429.

Kimmel, C. B., Ballard, W. W., Kimmel, S. R., Ullmann, B. and Schilling, T. F. (1995). Stages of embryonic development of the zebrafish. *Dev. Dyn.* **203**, 253-310.

Kimmel, C. B., Sepich, D. S. and Trevarrow, B. (1988). Development of segmentation in zebrafish. *Development* **104**, 197-207.

Korzh, V., Sleptsova, I., Liao, J., He, J. and Gong, Z. (1998). Expression of zebrafish bHLH genes *ngn1* and *nrd* defines distinct stages of neural differentiation. *Dev. Dyn.* **213**, 92-104.

Koshida, S., Shinya, M., Mizuno, T., Kuroiwa, A. and Takeda, H. (1998). Initial anteroposterior pattern of the zebrafish central nervous system is determined by differential competence of the epiblast. *Development* **125**, 1957-1966.

Kozak, M. (1987). An analysis of 5′-noncoding sequences from 699 vertebrate messenger RNAs. *Nucl. Acids Res.* **15**, 8125-8148.

McGrew, M. J., Dale, J. K., Fraboulet, S. and Pourquié, O. (1998). The *lunatic fringe* gene is a target of the molecular clock linked to somite segmentation in avian embryos. *Curr. Biol.* **8**, 979-982.

Makita, R., Mizuno, T., Koshida, S., Kuroiwa, A. and Takeda, H. (1998). Zebrafish *wnt11*: pattern and regulation of the expression by the yolk cell and No tail activity. *Mech. Dev.* **71**, 165-176.

Müller, M., von Weizsäcker, E. and Campos-Ortega, J. A. (1996). Expression domains of a zebrafish homologue of the *Drosophila* pair-rule gene *hairy* correspond to primordia of alternating somites. *Development* **122**, 2071-2078.

Oka, C., Nakano, T., Wakeham, A., de la Pompa, J. L., Mori, C., Sakai, T., Okazaki, S., Kawaichi, M., Shiota, K., Mak, T. W. and Honjo, T. (1995). Disruption of the mouse *RBP-J kappa* gene results in early embryonic death. *Development* **121**, 3291-301.

Orr-Urtreger, A., Givol, D., Yayon, A., Yarden, Y. and Lonai, P. (1991). Developmental expression of two murine fibroblast growth factor receptors, *flg* and *bek*. *Development* **113**, 1419-1434.

Primmett D. R., Stern, C. D. and Keynes, R. J. (1988). Heat shock causes repeated segmental anomalies in the chick embryo. *Development* **104**, 331-339.

Palmeirim, I., Henrique, D., Ish-Horowicz, D. and Pourquié, O. (1997). Avian *hairy* gene expression identifies a molecular clock linked to vertebrate segmentation and somitogenesis. *Cell* **91**, 639-648.

Roy, M. N., Prince, V. E. and Ho, R. K. (1999). Heat shock produces periodic somitic disturbances in the zebrafish embryo. *Mech. Dev.* **85**, 27-34.

Saga, Y. (1998). Genetic rescue of segmentation defect in MesP2-deficient mice by *MesP1* gene replacement. *Mech. Dev.* **75**, 53-66.

Saga, Y., Hata, N., Kobayashi, S., Magnuson, T., Seldin, M. F. and Taketo, M. M. (1996). MesP1: a novel basic helix-loop-helix protein expressed in the nascent mesodermal cells during mouse gastrulation. *Development* **122**, 2769-2778.

Saga, Y., Hata, N., Koseki, H. and Taketo, M. M. (1997). *Mesp2*: a novel mouse gene expressed in the presegmented mesoderm and essential for segmentation initiation. *Genes Dev.* **11**, 1827-1839.

Saitou, N. and Nei, M. (1987). The neighbor-joining method: a new method for reconstructing phylogenetic trees. *Mol. Biol. Evol.* **4**, 406-425.

Sparrow, D. B., Jen, W. C., Kotecha, S., Towers, N., Kintner, C. and Mohun, T. J. (1998). *Thylacine 1* is expressed segmentally within the paraxial mesoderm of the *Xenopus* embryo and interacts with the Notch pathway. *Development* **125**, 2041-2051.

Stachel, S. E., Grunwald, D. J. and Myers, P. Z. (1993). Lithium perturbation and *goosecoid* expression identify a dorsal specification pathway in the pregastrula zebrafish. *Development* **117**, 1261-1274.

Stern, C. D. and Keynes, R. J. (1987). Interactions between somite cells: the formation and maintenance of segment boundaries in the chick embryo. *Development* **99**, 261-272.

Talbot, W. S., Trevarrow, B., Halpern, M. E., Melby, A. E., Farr, G., Postlethwait, J. H., Jowett, T., Kimmel, C. B. and Kimelman, D. (1995). A homeobox gene essential for zebrafish notochord development. *Nature* **378**, 150-157.

Takada, S., Stark, K. L., Vassileva, G. and McMahon, J. A. (1994). *Wnt-3a* regulates somite and taibud formation in the mouse embryo. *Gene Dev.* **8**, 174-189.

Tam, P. P. and Trainor, P. A. (1994). Specification and segmentation of the paraxial mesoderm. *Anat. Embryol. Berl.* **189**, 275-305.

van Eeden, F. J., Granato, M., Schach, U., Brand, M., Furutani-Seiki, M., Haffter, P., Hammerschmidt, M., Heisenberg, C. P., Jiang, Y. J., Kane, D. A., Kelsh, R. N., Mullins, M. C., Odenthal, J., Warga, R. M., Allende, M. L., Weinberg, E. S. and Nüsslein-Volhard, C. (1996). Mutations affecting somite formation and patterning in the zebrafish, *Danio rerio*. *Development* **123**, 153-164.

van Eeden, F. J., Holley, S. A., Haffter, P. and Nüsslein-Volhard, C. (1998). Zebrafish segmentation and pair-rule patterning. *Dev. Genet*. **23**, 65-76.

Weinberg, E. S., Allende, M. L., Kelly, C. S., Abdelhamid, A., Murakami, T., Andermann, P., Doerre, O. G., Grunwald, D. J. and Riggleman, B. (1996). Developmental regulation of zebrafish *MyoD* in wild-type, *no tail* and *spadetail* embryos. *Development* **122**, 271-280.

Westin, J., Lardelli, M. (1997). Three novel *Notch* genes in zebrafish: implications for vertebrate *Notch* gene evolution and function. *Dev. Genes Evol.* **207**, 51-63.

Yamaguchi, T. P., Conlon, R. A. and Rossant, J. (1992). Expression of the fibroblast growth factor receptor FGFR-1/flg during gastrulation and segmentation in the mouse embryo. *Dev. Biol.* **152**, 75-88.

Yamaguchi, T. P., Harpal, K., Henkemeyer, M. and Rossant, J. (1994). *fgfr-1* is required for embryonic growth and mesodermal patterning during mouse gastrulation. *Genes Dev.* **8**, 3032-3044.

Yamamoto, A., Amacher, S. L., Kim, S. H., Geissert, D., Kimmel, C. B. and De Robertis, E. M. (1998). Zebrafish *paraxial protocadherin* is a downstream target of *spadetail* involved in morphogenesis of gastrula mesoderm. *Development* **125**, 3389-97.

Zhang, N. and Gridley, T. (1998). Defects in somite formation in *lunatic fringe*-deficient mice. *Nature* **394**, 374-377.